

# Development of a non-supervised and automatic method for detecting land cover changes in urban areas by using radar and optic data

Saeid Mahmoudizadeh<sup>1</sup>, Ali Esmaily\*<sup>1</sup>

<sup>1</sup>Department of Surveying Engineering, Graduate University of Advanced Technology, Kerman, Iran

## Article history:

Received: 4 February 2019, Received in revised form: 25 August 2019, Accepted: 12 September 2019

## ABSTRACT

Collecting updated and accurate land cover changes in urban areas have a significant impact on urban planning and management. In recent decades, remote sensing data have been used as valuable sources for detecting land cover changes. Given the different information that optical and radar sensors have received from any phenomenon on earth's surface, remote sensing data are assumed as complementary tools, and the integration of these two kinds of data will improve the results in detecting changes, especially in urban areas. In this research, a non-supervised and automatic method was developed to improve the detection of land cover changes in urban areas by integrating radar and optics data. Different spectral indices and radar polarizations were used to develop the CVA technique, known as an efficient non-supervised method for detecting the variations. In the implementation section, Sentinel 1 and 2 satellite data were used for the period of 2106 to 2018, captured from the northwest of Mashhad city, Iran. The developed technique was compared with other change detection methods. The findings of this study indicated the effectiveness and accuracy of the developed technique for detecting the changes. The estimated ratio of detected pixels to total pixels was 82%, which was promising. The overall classification accuracy and the kappa coefficient with values of 90.17 and 0.8016 were highest among the other methods used in the present study. The non-supervised approach and the verification results of the proposed method revealed its usefulness in detecting the changes, especially in urban areas.

## KEYWORDS

Change Detection  
Image Fusion  
Radar Polarization  
Otsu  
Change Vector Analysis

## 1. Introduction

The daily increase in urban population, as well as rural migrations, necessitates investigating and monitoring the urban changes in order to investigate the physical expansion of cities and environmental degradation and prevention of the immethodical development of cities (Nimrouzi, 2006). For monitoring, analyzing, planning, and management of urban areas, the comprehensive and precise information is required to make decisions in presenting services and facilities and also avoiding illegal constructions and expansion (Jantz et al., 2003).

Remote sensing is considered one of the modern, rapid, and low-cost techniques for obtaining the proper information at different levels for urban management. Different techniques

have been developed to extract the changes from multi-temporal satellite images-based data. Generally, change detection techniques can be divided into two groups of supervised and unsupervised. Supervised change detection, which is based on the supervised classification methods, requires some training data to train the classification algorithm. In addition to the detection of changing areas, this technique is able to determine the type of changes and compare one to another. The advantage of this method is its high strength in various atmospheric and optical conditions at different acquisition times. On the other hand, collecting the training data is usually considered as a disadvantage because it is time-consuming and very expensive. Therefore, over the past few years, developing unsupervised methods has become more popular because of the unnecessary in using

\* Corresponding author

E-mail addresses: [saedmahmodizadeh@gmail.com](mailto:saedmahmodizadeh@gmail.com) (S. Mahmoudizadeh); [aliesmaaily@kgut.ac.ir](mailto:aliesmaaily@kgut.ac.ir) (A. Esmaily)

DOI: 10.22059/eoge.2020.288831.1062

the training data. The resulted map from the unsupervised methods is converted into the binary map using the thresholding techniques. It displays the changed and unchanged areas and does not provide any information about the kind of changes. The high speed and low cost of this method can be mentioned as its advantages, while its high sensitivity to the imaging conditions can be considered as its disadvantage (Radke, 2005; Sallaba, 2009; Chen et al., 2012; Silva & Clarke, 2002). The urban areas are considered complex landscapes because of having different phenomena, diverse land covers, shapes, and patterns (Mhangara & Odindi, 2013; Xie, Fu, 2011). Principally, the optical and radar images are independently used to analyze the land surface changes, but considering the complexity of these areas, it is possible that some changed areas would not be detected if only one sensor was used. By considering the different information that these two sensors record for each land surface phenomenon, they could be a complement for each other. Therefore, by combining these two kinds of data (radar and multispectral), the detection of the changed areas will improve (Karimi et al., 2016). Using the radar data is highly popular because of its independency to solar and atmospheric conditions. In fact, the radar data present some information about the spatial and geometric features of the terrain, while the optical sensors are sensitive to the reflectance of objects at visible and infrared wavelengths, hence the surface reaction is different in the optical and radar data. The use of radar data in urban areas is restricted because of the dependency of the intensity data on the incidence angle and speckle noise.

On the other hand, only using the optical data in urban areas cannot present the accurate results because of the spectral similarity of the objects and an increase in the background noise. In addition, in most cases, an increase in spatial resolution causes a decrease in the spectral resolution of images. This concludes when using only one of these data sources, the optimum results in obtaining information in urban areas could not be achieved. In fact, both data sources provide complementary information of each other; thus their nature is different. Therefore, the fusion of both datasets would improve and increase the accuracy in obtaining the required information in urban areas (Ramezani & Sahebi, 2012; Ghanbari et al., 2012). Zeng et al. concluded that the feature fusion of radar and optic data is a suitable strategy to simplify the lack of information obtained independently by the sensors. For this reason, the radar and optical data were simultaneously used to detect the land surface changes in this research (Zeng et al., 2008). Mishra and Susaki proposed a simple and strong strategy to detect land cover changes using the combination of radar and optical data. The accuracy assessment revealed considerable improvement in detecting the changes. So far, the kappa coefficient was 0.73 in the optical image, 0.71 in the radar image, and 0.83 for the

combination of both data (Mishra & Susaki, 2014). Yousif and Ban presented the fusion of radar and optic images to detect the changes using unsupervised methods.

The fusion methods at decision-level and feature-level were investigated after classifying the images using the k-mean and support vector machine (SVM) methods. Their results showed higher accuracy of the decision-level compared to the feature-level (Yousif & Ban, 2017). Azzouzi et al. (2018) concluded that the radar images add additional and important information to the optical images, such as the soil moisture and roughness, which improve the results. Shokrelahi et al. (2014) tried to classify the San Francisco urban area using two fusion methods at the feature and decision levels for two data sources; RADARSAT2 and Hyperion. The results revealed that the classification accuracy would increase separately for each data source in both fusion methods.

In previous studies, various methods have been used and investigated to detect land cover changes using either single radar images or optic images and the combination of both data as well. The simultaneous use of radar and optic data in change detection has showed many advantages over using only one data source. However, the techniques implemented in the previous studies demonstrated some disadvantages and deficiencies when combining the radar and optic datasets. For instance, some methods used in some research works required to include a series of parameters or training data (supervised classification) by the operator. The skill and experience of the operator in determining these parameters and collecting the training data have an important effect on the results. However, the process is difficult and very expensive.

Another drawback emerges when the expansion of many thresholding techniques in one-dimensional space which are not appropriate for detecting the changes in the multispectral space. For this reason, the fusion of decisions and feature levels are used to resolve this setback.

In the present study, the main objective is to develop and implement an unsupervised and automated method for detecting urban changes and evaluating them by the fusion of optical and radar datasets. In the proposed method, the features of the optical and radar images were extracted and entered simultaneously in the CVA algorithm. After estimating the magnitude of the change, the changed and unchanged regions were determined using the Otsu threshold technique. The proposed method generates a map of changes for all stages without the need for user interaction. The proposed technique was evaluated with other unsupervised change detection methods using both optical and radar datasets either independently or simultaneously as well. These methods include the absolute value difference of the bands, the absolute magnitude difference of spectral indices, the application of the CVA method with optical and radar

data, the use of band ratio technique with the use of radar data, and the fusion at the decision level. In all of the above methods, the Otsu automatic threshold technique was used to determine the change maps.

**2. Theoretical foundations of the research**

In this section, we introduce the spectral features (spectral indices) used to detect the changes such as NDR<sup>1</sup>, change vector analysis (CVA), Otsu thresholding technique, and data fusion at the decision level.

**2.1. Spectral Index**

The spectral index is the result of a mathematical calculation between two or more spectral bands, by which the phenomenon becomes more pronounced. Table 1 shows how to calculate spectral indices; NDVI, SAVI<sup>2</sup>, ARVI<sup>3</sup>, NDBI<sup>4</sup>, and NDWI<sup>5</sup>, which are useful for studying and diagnosing three areas of efficient vegetation, water, and residential areas (Asadi et al., 2018).

**2.2. Change detection using radar data**

In radar images, due to the presence of speckle noise, it is better to use the ratio of the corresponding pixel values

instead of the difference of the two images. This is one of the methods for decreasing the noise effect in detecting the changes, specifically in the radar images because of the multiplication nature of the speckle noise. The ratio operator will have a better performance compared to difference operator (Khodayi et al., 2011; Najafi & Hasanlou, 2018). Eqs. (6) and (7) show how to calculate the difference and the ratio operators in an image in detecting the changes.

$$IR = A_{t2} - A_{t1} \tag{6}$$

$$ID = \frac{A_{t2}}{A_{t1}} \tag{7}$$

In these equations, t1 and t2 represent different times for taking the image from the same geographical region.

Mishra used Eq. (8) to normalize the image ratio operator. In this equation, the pixel values have the range of -1 to +1 and the space from the pixel values to zero demonstrates the changes (Mishra & Susaki, 2014).

$$NDR(t1,t2) = \frac{A_{t2} - A_{t1}}{A_{t2} + A_{t1}} \tag{8}$$

Table 1. Spectral Indices

Equation number	Index	Description
1	$NDVI = \frac{NIR - RED}{NIR + RED}$	NIR is the reflection value in the near-infrared band and RED is the reflection value in the red band.
2	$SAVI = \frac{(NIR - RED)(L + 1)}{(NIR + RED + L)}$	L is the factor of correcting the soil effects, which varies in the range of 0 to 1. L would be 1 if the vegetation is sparse, and it is 0.5 when the vegetation is denser and will trend to 0 for highly dense vegetation.
3	$ARVI = \frac{(NIR - (2 * RED - BLUE))}{(NIR + (2 * RED - BLUE))}$	Blue is the reflection value in the blue band.
4	$NDBI = \frac{SWIR - RED}{SWIR + RED}$	SWIR is the reflection value in the short wave infrared band.
5	$NDWI = \frac{GREEN - NIR}{GREEN + NIR}$	GREEN is the reflection value in the green band.

<sup>1</sup> Normalized difference ratio

<sup>2</sup> Soil adjusted vegetation index

<sup>3</sup> Atmospherically resistant vegetation index

<sup>4</sup> Normalized Difference Built-up Index

<sup>5</sup> Normalized difference water index

### 2.3. Change Vector Analysis (CVA)

The change vector analysis method is considered as one of the most appropriate methods for detecting the changes as well as determining the magnitude of the changes. In addition, it has the capacity to determine the direction of changes (Malila, 1980). In 2012, Bovolo et al. (2012) proposed the C<sup>2</sup>VA theory, which was the developed CVA method, to maintain the information in all spectral bands and use them simultaneously [Eqs. (9) and (10)].

$$M = \sqrt{\sum_{i=1}^n x_{diff}^2} \quad (9)$$

$$a = \cos^{-1} \left[ \frac{1}{\sqrt{n}} \left( \frac{\sum_{i=1}^n x_{diff}}{\sqrt{\sum_{i=1}^n x_{diff}^2}} \right) \right] \quad (10)$$

In the above equations,  $m$  and  $a$  represent the magnitude and direction of changes, respectively.  $X_{diff}$  is the difference of a band taken at times  $t_1$  and  $t_2$  and  $I$  is the number of spectral bands. The change range of  $m$  and  $a$  can be represented as follows.

$$C^2VA = \{m \in [0, \max(m)] \text{ and } \alpha \in [0, \pi]\} \quad (11)$$

By indicating a threshold, the output of  $m$  can be divided into two classes ( $\Omega$ ,  $\omega$ ), which will represent the changed and unchanged pixels respectively. The changed class will consist of a subset for all created changes.

$$\omega = \{m, \alpha : 0 \leq \rho < T \text{ and } 0 \leq \alpha \leq \pi\} \quad (12)$$

$$\Omega = \{m, \alpha : T \leq \rho \leq \rho_{max} \text{ and } 0 \leq \alpha \leq \pi\} \quad (13)$$

### 2.4. Thresholding technique

One of the methods used to detect the changes in the difference images is the thresholding technique. If a multispectral image is taken from the same geographical area at times  $t_1$  and  $t_2$  and are represented by two vectors  $X_1$  and  $X_2$ , one will have:

$$X_1 = [x_1, \dots, x_b] \quad (14)$$

$$X_2 = [x_1, \dots, x_b] \quad (15)$$

In the above equation,  $b$  is the number of spectral bands. The difference of two vectors presents the pixel change rate in each spectral band.

$$XD_1 = X_1 - X_2, \dots, XD_b = X_1 - X_2 \quad (16)$$

By applying a threshold to  $XD$  values, the separation of the changed and unchanged areas will be possible. In spite of the

simplicity of this technique, thresholding methods can always have some difficulties, and the middle value is determined through the trial and error method. In this research, the Otsu threshold was used to determine the optimum threshold for determining the changed and unchanged classes. This technique will be explained in the following section (Otsu, 1979).

#### 2.4.1. Otsu thresholding

This method is an effective technique to select the optimum threshold automatically by maximizing the variance between the classes and minimizing the variance inside the pixel classes. In other word, it maximizes the separation of the changed pixels ( $C_1$ ) and the unchanged pixels ( $C_0$ ) considering the variance of the related classes.

The image obtained from the absolute value of the difference between two bands can be considered as an intensity function which consists of  $N$  pixels with the gray-levels between 1 and  $L-1$ . If the number of pixels with gray-level  $i$  is displayed by  $f_i$ , the following Eq. (17) is the probability of gray-level  $i$  in the image obtained from the absolute value of the difference between two bands.

$$P_i = \frac{f_i}{N} \quad (17)$$

If the optimal threshold is shown by  $t$ , the class of unchanged pixels  $C_0$  is the sum of probabilities in the gray-levels  $[1, \dots, t]$ , and the class of changed pixels  $C_1$  is the sum of probabilities in the gray-levels  $[t + 1, \dots, L]$ . Therefore, the gray-level probability distribution in two changed and unchanged classes is as follows [Eq. (18) and (19)].

$$C_0 = \frac{P_1}{W_0(t)}, \frac{P_2}{W_0(t)}, \frac{P_3}{W_0(t)}, \dots, \frac{P_t}{W_0(t)} \quad (18)$$

$$C_1 = \frac{P_{t+1}}{W_1(t)}, \frac{P_{t+2}}{W_1(t)}, \frac{P_{t+3}}{W_1(t)}, \dots, \frac{P_{L-1}}{W_1(t)} \quad (19)$$

After calculating the probability of both changed and unchanged classes ( $w_0(t) \cdot w_1(t)$ ) using Eqs. (20) and (21). Eqs. (22) and (23) are used to calculate the average of the two considered classes.

$$w_0(t) = \sum_{i=1}^t P_i \quad (20)$$

$$w_1(t) = \sum_{i=t+1}^{L-1} P_i \quad (21)$$

<sup>6</sup> Compressed CVA

$$\mu_0(t) = \sum_{i=1}^t i \frac{P_i}{W_0(t)} \quad (22)$$

$$\mu_1(t) = \sum_{i=t+1}^{L-1} i \frac{P_i}{W_1(t)} \quad (23)$$

Consequently, the optimum threshold in the Otsu technique is introduced as the following equation:

$$t = \text{Arg Max} \{w_0(t) * [\mu_0(t)]^2 + w_1(t) * [\mu_1(t)]^2\} \quad (24)$$

$$1 \leq t \leq L-1$$

### 2-5. Data Fusion techniques

In the present study, two methods have been used to synthesize the radar and optic data in order to improve change detection in urban areas. The first method is the Fusion technique at the decision-level, and the second method (the proposed method), considered as the combined level, uses a simultaneous combination of two different fusion levels (Fusion at pixel-level and fusion at feature-level) and will be explained in detail in the methodology section (3.3.1).

#### 2.5.1. Data Fusion technique at decision level

At this level of data synthesis, which is introduced as the highest level of the data synthesis, after processing the data, some of their information is extracted and merged together using some rules at the decision level. At this level, it is possible to synthesize different data obtained by various sensors. Data classification is one of the most efficient processes of decision-making in order to identify and extract the terrain. However, the use of only one classifier is not appropriate. On the other hand, considering the different results provided by various classifications and the simultaneous use of diverse classifiers will improve the results. For this reason, some methods have been presented to merge the classifiers, of which the most efficient is the merge at the decision level. The objective of this technique is to use the decisions of multiple classifiers simultaneously and synthesize them for improving the results. One of the most common methods for merging the classifiers at the decision level is the Voting Method which has an unsupervised implementation (Samadzadegan et al., 2014).

Zhang et al. (2010) determined two changed and unchanged classes using the following conditions to synthesize the difference of n spectral bands whose optimum threshold has been determined [Eq. (25)].

$$\begin{aligned} &\text{if } x_1(i,j) \leq t_1 \ \& \ x_2(i,j) \leq t_2 \ \& \ \dots \ x_n(i,j) \leq t_n \\ &x(i,j) \in C_0 \\ &\text{else } x(i,j) \in C_1 \end{aligned} \quad (25)$$

In the above equation,  $x_i(i,j)$  is the difference between the image bands at different times in n spectral bands.

## 3. Materials and research method

### 3.1. Study area

Mashhad is a metropolis in the northeast of Iran, and it is the capital city of the Khorasan Razavi province. The city is located in the longitude 59°15' to 60°36' and the latitude 35°43' to 37°8' (Figure 1a). The study area is a region in the northwest of this city, and significant land cover changes have been observed between 2016 and 2018 (Figure 1b).

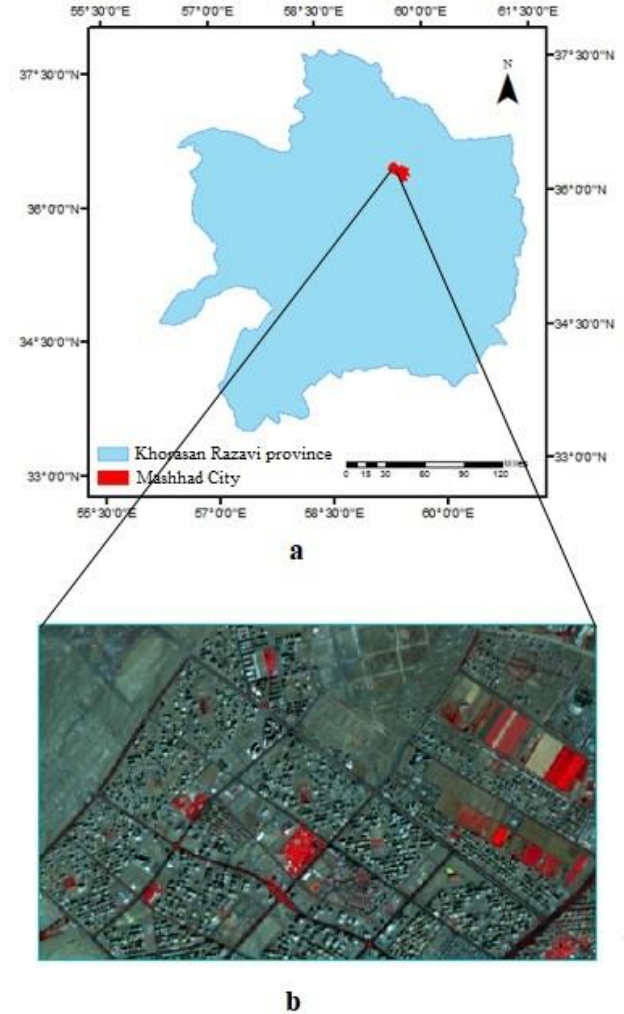


Figure 1. (a) Position of the study area, (b) Aerial image with a false color combination from the study area

### 3.2. Data analysis

The dataset used to evaluate the proposed method is a pair of multispectral images acquired by Sentinel 2 satellite in September 2016 and September 2019 and also two SAR images of Sentinel 1 satellite acquired in September 2016 and September 2018 over the study area (Figure 2). Sentinel 2 satellite has 13 spectral bands in the ranges of visible, near infrared, and short wave infrared (SWIR). The spatial resolution for four visible bands (Blue, Green, Red, NIR) is 10 meters, while for the SWIR bands it is 20 meters. Sentinel 1 satellite is a sun synchronous satellite with a SAR

imaging system, which captures the images in band C. Its data are offered in two polarizations of VV and VH with a spatial resolution less than 10 meters. In this research, both of the polarizations have been used.

In this research, the Envi software was used for most of the processing. However, the Snap software was employed to preprocess the radar images.

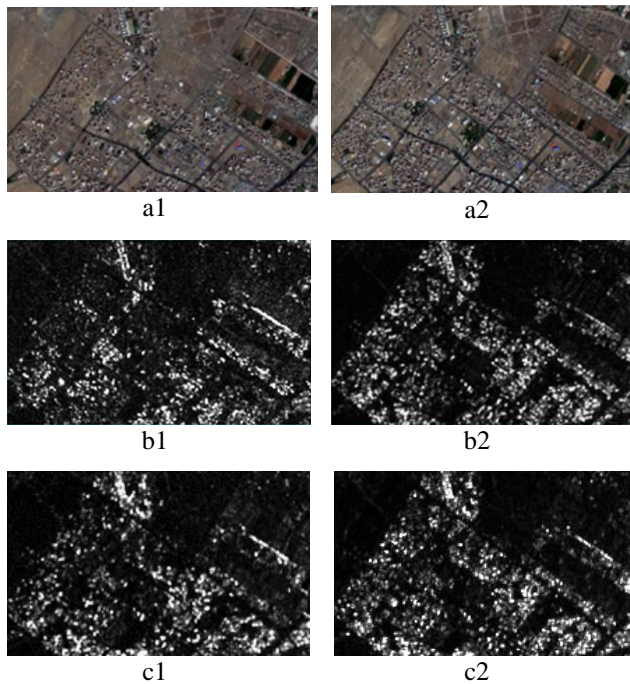


Figure 2. Used data, (a) Sentinel-2 images acquired in 2016 and 2018, (b) Sentinel-1 images acquired in VV polarization in 2016 and 2018 and, (c) Sentinel-1 images acquired in VH polarization in 2016 and 2018

### 3.3. Research method

#### 3.3.1. Pre-processing

When using satellite images to detect the changes, the preprocessing stage of these images is very important. Preprocessing is often included as decreasing image dimensions, changing the pixel sizes, geometric corrections, and radiometric corrections. Since the coordinate system in sentinel-2 data is predefined, the geometric correction is not necessary. However, considering the simultaneous use of SWIR and visible bands, having a similar spatial resolution is required. Therefore, by using the nearest-neighbor interpolation approach, the 20-meter pixel size of the SWIR band was resampled to 10 meters following with a histogram matching algorithm for radiometric correction. For the last case, using the histogram of the reference image, the histogram of the target image is changed in such a way that the radiometric properties of two similar images and the differences between gray-level values of two images were decreased. In the preprocessing stage of radar images,

geometric corrections were applied to the images followed by applying the radiometric correction using a DEM of the region. Afterward, the filter Enhanced Lee with the kernel size  $3 \times 3$  was used to remove the speckle noise. Now, because of the difference in spatial resolution of Radar and optic data, they should be brought to the same resolution. This explains why the nearest neighbor approach was employed to obtain the 10-meter spatial resolution for all of the data. The final stage of this section would be the registration of radar images relative to the optic images to match them geometrically.

In the detection process, the accuracy of image registration will have a significant impact on the accuracy of the outputs. If accurate registration between images could not be achieved, then false differences will be detected. This will be doubled in urban areas due to numerous complications. The methods used in this study were pixel-based and identified the changes based on the smallest unit of pixels. Therefore, matching the pixels of the images to each other is important. So, we tried to match the images with the best accuracy to minimize the negative impact on the outputs. Townshend et al. (1992) investigated the accuracy of registering low and medium spatial resolution images in output maps and concluded that in areas with dense vegetation, registering images with one-pixel accuracy results in 50% false pixels. In order to improve the results of less than 10%, it should be registered at the resolution of 0.2-pixel. This will be less than 0.5-pixel accuracy for the areas with low vegetation. When using high-resolution images, one typically experiences a high spectral variation in neighboring pixels compared to low-resolution images, especially in urban areas, due to a variety of phenomena. As a result, accurate image registration is crucial for discussing change detection, even when using object-based methods (Chen et al., 2014).

#### 3.3.2. Proposed method

The flowchart in Figure 3 presents the proposed method in detail, and all steps, including implementation and change detection methods, are explained. In the first step, the absolute value image of the difference between the described bands was calculated, and each one was divided into two changed and unchanged classes using the Otsu threshold technique. Then, the  $C^2VA$  method was used to calculate the magnitude of the change ( $m$ ), using five spectral bands (Blue, Green, Red, NIR, SWIR) and the changed and unchanged areas were determined using the Otsu thresholding technique. In the next step, a series of spectral features were extracted from different bands of images taken at the two mentioned dates, and their absolute value difference was calculated. Afterward, the Otsu threshold method was used to determine the threshold in the image of the absolute value difference. The spectral features used in this research consist of the spectral indices such as NDVI, SAVI, ARVI, NDBI NDWI. Subsequently, all the extracted spectral indices were

entered in the  $C^2VA$  algorithm, and the Otsu threshold was used to separate two classes after calculating the change magnitude parameter. For detecting the changes using radar images, the changed and unchanged areas were first separated using an NDR operator for two polarizations VV and VH, and then the Otsu technique was applied. Thus, the normalized difference ratio (NDR) images calculated from polarizations VV and VH, were entered in  $C^2VA$  algorithm, and after calculating the parameter M using the Otsu threshold technique, it was divided into two changed and

unchanged classes. In the next stage, the optic and radar data were merged to detect the changes. Accordingly, the data fusion technique at the decision-level was applied [Eq. (25)]. The input of this method is two binary images obtained from the output of the  $C^2VA$  algorithm. In fact, the algorithm was applied once on the spectral index and then on the normalized difference ratio images (polarized images). Another method to merge the radar and optic data will be explained in the following section, which is our proposed method to improve the change detection.

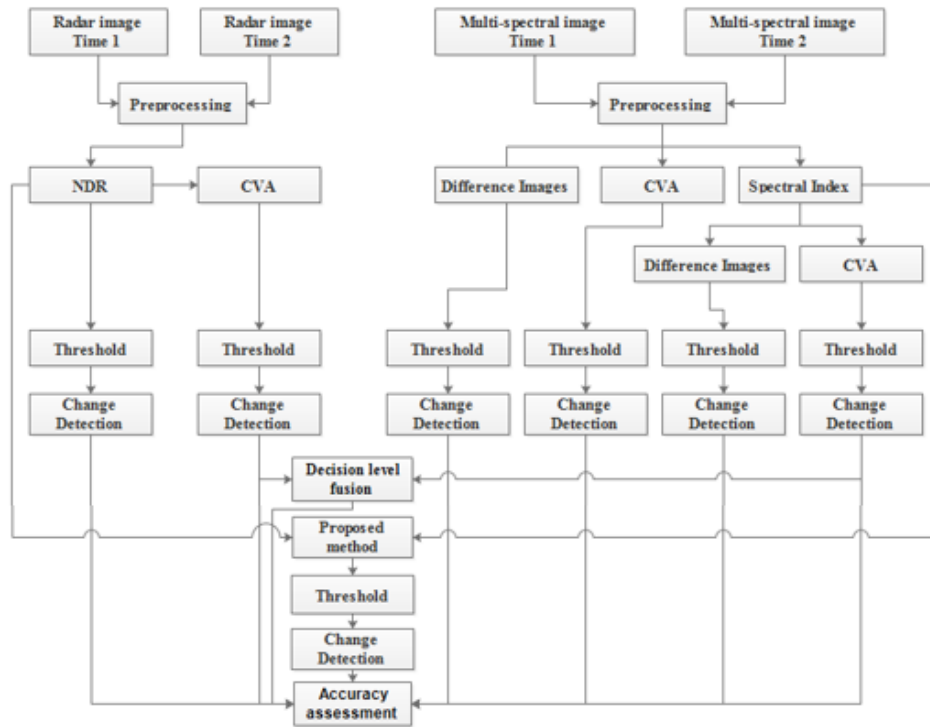


Figure 3. Research method flowchart

### 3.3.3. Implementing the proposed method

The proposed method was used as a technique for the fusion of radar and optic datasets for obtaining a single-band image. This technique is a simple and usable solution for data fusion and for reducing the dimension of data from n to one. This method can be considered as a fusion method at the combined level because it has been used from the simultaneous combination of two different fusion levels (Fusion at pixel-level and fusion at feature-level).

In the fusion of data at the pixel-level, the signals recorded by different sensors are combined pixel-by-pixel with each other after being converted to an image. And the purpose of this procedure is to increase the information of each pixel, but fusion at the feature-level requires the extraction of needed features from different data, which are finally fused together using the appropriate techniques. In the proposed method, the features extracted from the optic and radar images are fused together pixel-by-pixel.

For the fusion of these features with the objective of detecting the changes, the  $C^2VA$  technique was used as explained in section 3-2. This technique gives the possibility of data fusion at the pixel-level to increase the information content of each pixel. Generally, the input of this method is divided into two categories of radar and optical data. For reducing the effects of the topography and image brightness and increasing the possibility of detecting and separating the terrain, the spectral indices were used as an input of the optic section. The spectral indices extracted from the bands of images acquired at times t1 and t2 consists of NDVI, SAVI, ARVI, NDWI, NDBI, which are effective in studying and detecting in three fields of vegetation, water, and residential regions. The input of radar data is the normalized difference ratio images acquired from polarizations VV and VH provided by the radar sensor at times t1 and t2. The output of

this technique will be a single-band image where its pixels represent the intensity or magnitude of the changes (m). Ultimately, the Otsu threshold technique was used to determine the image threshold and divide it into two changed and unchanged classes that are unsupervised.

Finally, in order to evaluate the accuracy of the produced binary maps, all the explained methods were compared to the ground truth data, and five evaluation parameters including the percentage of the changed pixels placed in the unchanged class, the percentage of unchanged pixels located in the changed class, the ratio of identified false pixels to the total pixels of the evaluation data, the overall classification accuracy and finally, the kappa coefficient were estimated using the error matrix.

#### 4. Results and discussion

In the first step of this research, the two different sources of data needed to be matched. In order to register the images, appropriate control points were selected from areas such as road corners and road intersections at image surfaces and by using the mathematical model of the second degree polynomial. The accuracy of registration is usually quoted in terms of the root mean square (rms) error of the location of ground control points. Values of 0.5 to 1.0 pixels are normally considered satisfactory; however, visually checking the results by overlaying two images is also a very good approach to make sure if the registration is acceptable. The results of this part showed an accuracy of 0.5 pixels in the registration of data, which is acceptable to continue the rest of the research.

After providing the required preprocessing of the optic and radar data, the methods represented in the flowchart were used to identify the changed areas. Figure 4 displays the output of these methods divided into two changed and unchanged classes using the Otsu thresholding technique. For quantitatively evaluating the obtained results, all the achieved outputs were compared to the ground truth data, and after calculating the error matrix, five evaluation parameters including the percentage of changed pixels placed in the unchanged class, the percentage of unchanged pixels located in the changed class, the ratio of identified false pixels to the total pixels of the evaluation data, the overall classification accuracy and finally, the kappa coefficient were calculated, and the obtained result was represented in Table 2 and Figures 5-7.

The output of the absolute value difference in the bands SWIR, NIR, Red, Green and Blue whose average

wavelengths are 0.49, 0.56, 0.65, 0.84 and 0.61, respectively were divided into two changed and unchanged classes after applying the Otsu threshold technique (images 1-5 of Figure 4). Visual comparison of the binary images of this section represents that the changes of the land surface cover will be detectable using different wavelengths and in different bands of the multispectral image of the optic sensors. Considering the quantitative evaluation of the binary images produced based on the absolute difference method of the spectral bands, the binary image obtained from band 3 (Red) has greater accuracy compared to other bands, and in this image, the percentage of changed pixels placed in the unchanged class is equal to 39.64%, the percentage of unchanged pixels placed in the changed class is equal to 22.13%, and the ratio of identified false pixels to the total pixels of the evaluation data is equal to 30%. Thus, they have smaller values compared to other spectral bands.

Images obtained from the absolute value difference technique of the spectral indices (NDVI, SAVI, ARVI, NDWI, NDBI) divided into two changed and unchanged classes using the Otsu thresholding technique, as depicted in images 6-10 of Figure 4. Considering the noise reduction when using the spectral index, the overall accuracy of detecting the changes will be greater, and the number of false detected pixels will be fewer. The quantitative result evaluation of this section and their comparison to the values presented for the absolute difference images of the spectral bands can support this idea. Among the used indices, NDBI has a lower accuracy (the number of false detected pixels is greater) compared to other used indices, because of the spectral disturbance in band 11, which happened due to a reduction in the spatial resolution from 20 meters to 10 meters.

The changed areas determined using the NDR technique with the polarizations VV and VH of radar images have been depicted in images 11 and 12 of Figure 4. By comparing the results and quantitative evaluation, it can be concluded that the technique implemented based on SAR images, especially for polarization VH, has a lower accuracy for detecting the changes compared to the techniques used based on optic images. Therefore, in binary images produced based on polarization VH, the percentage of changed pixels placed in the unchanged class is equal to 97.85%, the percentage of unchanged pixels placed in the changed class is equal to 4.45%, and the ratio of detected false pixels to the total pixels of the evaluation data is equal to 46.40%.

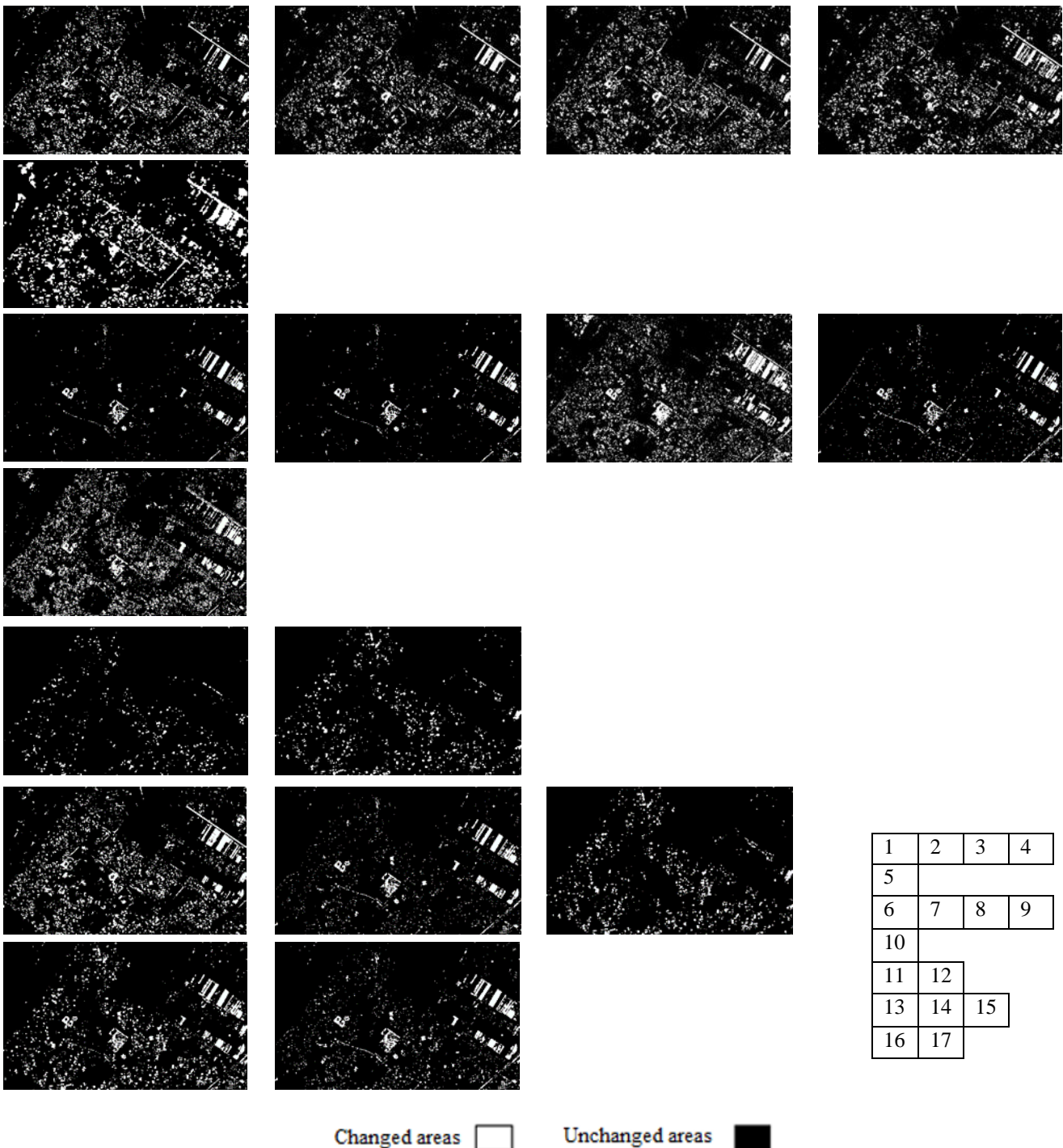


Figure 4. Images 1-5 are binary images obtained by determining the threshold of absolute value difference images in the bands Blue, Green, Red, NIR, and SWIR; images 6-10 are binary images obtained by determining the threshold of absolute value difference images in the spectral Index NDVI, SAVI, ARVI, NDWI, and NDBI; images 11-12 are binary images obtained by determining the threshold of NDR images with polarizations VV and VH; image 13 is a binary image obtained through determining the threshold of the change magnitude image obtained from  $C^2VA$  technique by using all spectral bands; image 14 is a binary image obtained from determining the threshold of the change magnitude image obtained from  $C^2VA$  technique by using all spectral Index; image 15 is a binary image obtained by determining the threshold of the change magnitude image obtained from  $C^2VA$  technique using the polarizations VV and VH; image 16 is a binary image obtained by synthesizing images 14 and 15 at the decision-level using Eq. (25); and image 17 is a binary image obtained by determining the threshold of the image obtained from the proposed method.

Table 2. Results of verifying change detection techniques

method			Changed pixels located in unchanged class	Unchanged pixels located in changed class	Ratio of identified false pixels to the total pixels of evaluation data	Overall classification accuracy	Kappa coefficient
Absolute value difference	Spectral bands	Blue	48.046	25.636	35.70	64.29	0.267
		Green	46.093	28.662	36.49	63.5	0.255
		Red	39.648	22.133	30	70	0.38
		NIR	43.945	21.178	31.403	68.59	0.354
		SWIR	45.703	23.885	33.684	66.14	0.3049
	Spectral indices	NDVI	32.617	3.025	16.315	83.68	0.6612
		SAVI	32.617	3.025	16.315	83.68	0.6612
		ARVI	30.273	6.847	17.368	82.63	0.6418
		NDWI	23.632	14.649	18.684	81.31	0.62
		NDBI	23.242	19.90	21.403	78.59	0.56
NDR	VH	97.851	4.458	46.403	53.59	0.025	
	VV	86.718	10.350	44.649	55.35	0.0315	
C <sup>2</sup> VA	VH, VV	87.890	6.847	43.245	56.75	0.056	
	5 spectral bands	35.742	21.019	27.631	72.45	0.438	
	Spectral index	23.242	6.68	14.122	85.87	0.7106	
Fusion of optic and radar data	Decision level	19.531	14.012	16.491	83.50	0.6666	
	Proposed method	10.546	9.235	9.824	90.17	0.8016	

As explained, different changes of the land surface cover are detectable in different parts of the electromagnetic spectrum; thus, the simultaneous use of all bands will improve the change detection. The C<sup>2</sup>VA technique has provided the possibility of using all spectral bands information at the same time to detect the changes. After applying the threshold, the output of this method, which is a compressed single-band image, is divided into two changed and unchanged classes. The binary images (13-15) in Figure 4 are the output of the C<sup>2</sup>VA method, which were generated

using the spectral bands, the spectral indices, and polarizations VV and VH, respectively. They also were divided into two changed and unchanged classes after applying the Otsu thresholding technique. By comparing the evaluated results, it was shown that the accuracy of this technique for detecting the changes was higher than the state in which the spectral bands, the spectral indices, and the radar polarizations were used separately. When the C<sup>2</sup>VA technique was used for utilizing all the spectral bands at the same time, the overall accuracy reached 72.45%, while using

the bands separately, the best obtained accuracy was related to band 3 (RED), and its overall accuracy was 70%. This outcome of comparison was also the same for the spectral indices and the radar polarizations. On the other hand, by using all the spectral indices and radar polarizations, the

overall accuracy raised to 85.88 and 56.75, respectively, which represent an improvement in detecting the changes, compared to the state that each index or polarization was used separately.

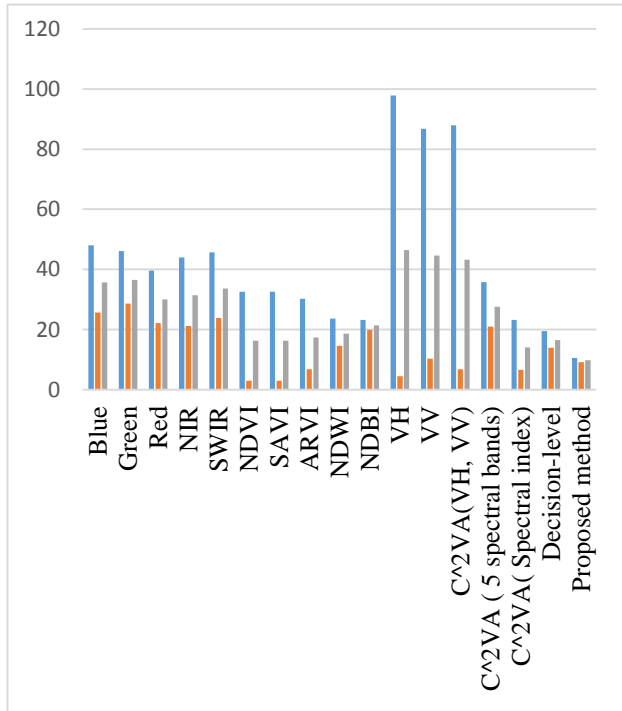


Figure 5. Result chart of verifying change detection techniques based on three parameters i.e., the percentage of changed pixels placed in the unchanged class (blue chart), the percentage of unchanged pixels placed in changed class (orange chart) and the ratio of detected false pixels to the total pixels of evaluation data (gray chart)

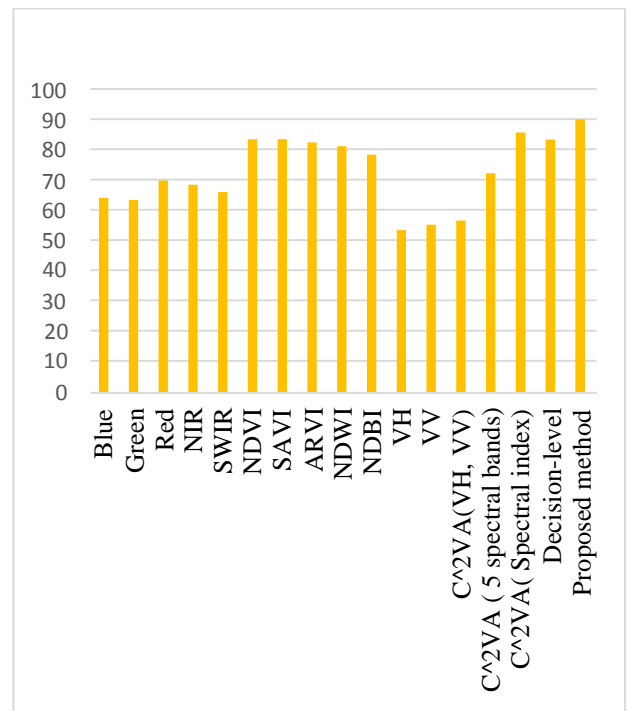


Figure 6. Result chart of verifying change detection techniques based on the overall classification accuracy parameter

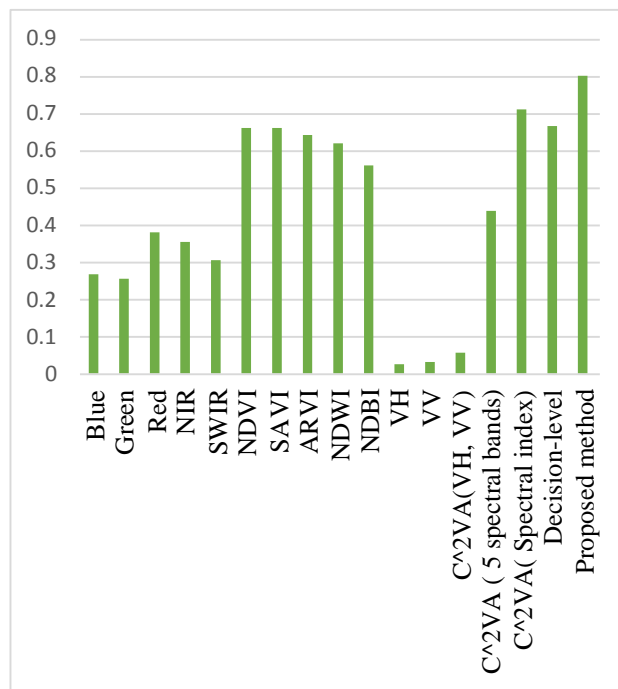


Figure 7. Result chart of verifying change detection techniques based on the Kappa coefficient parameter

Considering the different information recorded from the phenomena on the land surface using the optic and radar sensors, it was concluded that they are a complement for each other. Thus, integrating the data of both sensors will improve the accuracy of change detection areas. In this research, two fusion methods (Fusion at the decision-level and Fusion using the proposed method) were implemented to investigate the performance of synthesizing the optic and radar data for detecting the changes.

In the data fusion technique at the decision-level, the binary images were produced by applying the  $C^2VA$  technique. The spectral indices and radar polarizations were used, and both were merged together using the equation presented in section 2.5.1. The output of this method is displayed in image 16 of Figure 4. The visual evaluation of this output represents the aggregation of two binary images created with the help of the  $C^2VA$  technique using the spectral indices and radar polarizations. The quantitative evaluating of this technique represented in Table 2. A reduction in the percentage of the changed pixels placed in the unchanged class can be seen (19.53% versus 87.89 and 23.24), which represents an improvement in the change detection. On the other hand, the percentage of unchanged pixels placed in the changed class increased in this technique (14.012 compared to 6.48 and 6.68).

As a data fusion technique at the combined level, the proposed method was implemented in the present research to detect the land cover changes. The output of this method is represented in image 17 of Figure 4. In this technique, all spectral indices and normalized difference ratio images acquired from the radar polarizations were simultaneously entered in the  $C^2VA$  algorithm, and the output, as a single-band image, was divided into two changed and unchanged classes by applying the Otsu thresholding technique. In the mentioned method, the percentage of the changed pixels placed in the unchanged class was equal to 10.55%, which had a considerable reduction compared to other methods. This result can represent the high efficiency of this method in detecting the changed areas. Furthermore, the percentage of unchanged pixels placed in the changed class was 9.24%, which reduced in contrast to some methods of this research. The ratio of detected false pixels to the total pixels of the evaluation data for the proposed method was equal to 9.83%, which was the lowest value compared to other used methods. In addition to the three parameters, if one analyzed the overall accuracy and the kappa coefficient, it would show obviously that the proposed method with the overall accuracy 90.17 and the kappa coefficient 0.80 was placed at a higher level in comparison to the other used methods.

## 5. Conclusion

Considering the advantage of using the radar and optic data at the same time as well as using the unsupervised methods

in detecting the changes, this study tried to develop an unsupervised and automatic technique to integrate the radar and optic data for detecting the changes. Using the radar and optic data, the  $C^2VA$  technique can provide the possibility of synthesizing the data and also reducing the dimension of the data from  $n$  to one. The input of this technique consisted of two groups, i.e., the radar and optic data, and the optic data consisted of five spectral indices (NDVI, SAVI, ARVI, NDWI, and NDBI) which were extracted from Sentinel-2 images at two intervals in September 2016 and September 2018. The radar data consisted of the normalized difference ratio (NDR) images obtained from polarizations VV and VH of Sentinel-1 satellite at two intervals in September 2016 and September 2018. The output of this technique was divided into two classes of the changed and unchanged areas after applying the Otsu automatic thresholding. For evaluating the performance of the mentioned technique in the change detection, a set of the ground truth data and a comparison between the results of this technique with other unsupervised change detection methods were used.

These methods were including the absolute value difference in the spectral bands, the absolute value difference in the spectral index, the normalized difference ratio images obtained from the radar polarizations, the  $C^2VA$  method using the optic and radar data independently, and the fusion at the decision-level. The error matrix, which is a result of comparing the ground truth pixels and the corresponding pixels in the output of change detection methods, was used to estimate the five parameters for all the methods of this research: 1) the percentage of changed pixels placed in the unchanged class, 2) the percentage of unchanged pixels placed in the changed class, 3) the ratio of detected false pixels to the total pixels of the evaluation data, 4) the overall classification accuracy and 5) the Kappa coefficient.

The obtained results represent the high capacity of the proposed method in detecting the changed areas with high accuracy so that in the proposed method, the ratio of detected false pixels to the total pixels of the evaluation data was equal to 82.9% which had the smallest value. The overall classification accuracy and the Kappa coefficient were equal to 90.17 and 0.80 respectively, and they were considered as the greatest values compared to those of other methods used in the present study.

The mentioned technique is unsupervised, and it has high accuracy in detecting the changes, and these are considered as the most important advantages of the proposed method. Based on the obtained results and presented analyses, it can be concluded that the performed research was very successful in detecting the changes in urban areas.

## References

Azzouzi S.A., Pantaleoni A.V., & Bentounes H.A. (2018). Monitoring desertification in Biskra, Algeria using

- Landsat 8 and Sentinel-1A images, *IEEE Access*.
- Asadi, S., Bannayan, M., Jahan, M., & Faridhosseini, A. (2018). Comparison of Different Spectral Vegetation Index for the Remote Assessment of Winter Wheat Leaf Area Index in Mashhad. *Journal of Agroecology*, 10(3): 913-934.
- Bovolo, F., Marchesi, S., & Bruzzone, L. (2012). A framework for automatic & unsupervised detection of multiple changes in multitemporal images. *IEEE Trans. Geosci. Remote Sens.*, 50(6), 2196-2212.
- Chen, X., Chen, J., Shi, Y., & Yamaguchi, Y. (2012). An automated approach for updating land cover maps based on integrated change detection and classification methods. *ISPRS Journal of Photogrammetry and Remote Sensing*, 71, 86-95.
- Chen, G., Zhao, K., & Powers, R. (2014). Assessment of the image misregistration effects on object based change detection. *ISPRS Journal of Photogrammetry and Remote Sensing*. 87. 19-27. 10.1016/j.isprsjprs.2013.10.007.
- Ghanbari Alavijeh, Z., Sahebi, M.R., & Mohammadzadeh, A. (2012). Urban classification using the fusion of optical and SAR satellite images, A Thesis for Degree of Master of Science (M.Sc.) in Remote Sensing Engineering, *K.N. Toosi University of Technology Faculty of Geodesy and Geomatics*
- Jantz, C., Goetz, S., Smith, & Shelly, M. (2003). Using the SLEUTH Urban growth model to simulate the impacts of future policy scenarios on land use in the Baltimore Washington metropolitan area, *Environment and Planning*. 31(2):251-271.
- Karimi, D., Rangzan, K., Akbarizadeh, G., & Kabolizadeh, M. (2016). Ensemble classification of targets using SAR and optical data fusion, Thesis as requirement for the degree of M.Sc. in *Remote Sensing & GIS, Shahid Chamran University of Ahvaz, Faculty of Earth Sciences, Department of Remote Sensing & GIS*.
- Khodaei, B., Amini, J., & Momeni, M. (2011). Providing an unattended method for changes detection in SAR images by using a genetic algorithm. *Remote sensing and GIS of Iran*, 95-106.
- Malila, W.A. (1980). Change Vector Analysis: An Approach for Detecting Forest Changes with Landsat. *LARS Symposia*, 326-335.
- Mhangara, P., & Odindi, J. (2013). Potential of texture based classification in urban landscapes using multispectral aerial photos. *South African Journal of Science*, 109(3-4):1-8.
- Mishra, B. & Susaki, J. (2014). Optical and SAR data integration for automatic change pattern detection. *ISPRS Annals of the Photogrammetry, Remote Sensing and Spatial Information Sciences*, 3946.
- Najafi, A., & Hasanlou, M. (2018). Land cover changes detection in polarimetric SAR data using algebra, similarity, and distance based methods. *JGIT*. 6 (2) :143-163
- Nimrozi, M. (2006) Reviewing the consequences of marginalization on the cultural system of Mashhad, Mashhad Planning and Management Conference, Ferdowsi University, 73-88.
- Otsu, N. (1979). A threshold selection method from gray-level histogram. *IEEE Trans. Systems Man Cybernet*, 9, 62-66.
- Radke, R. J., Andra, S., Al-Kofahi, O., & Roysam, B. (2005). Image change detection algorithms: a systematic survey. *Image Processing, IEEE Transactions*. 14(3), 294-307.
- Ramezani, M.R. & Sahebi, M.R. (2013). Forest Biomass Estimation Using SAR and Optical Images. *JGIT*. 3 (1) :15-266.
- Samadzadegan, F., Tabib Mohmoudi, F., & Bigdeli, B. (2015). Data Fusion in Remote Sensing Concepts & Techniques. *University of Tehran Press*.
- Sallaba, F. (2009). Potential of a Post Classification Change Detection Analysis to Identify Land Use and Land Cover Changes. A Case Study in Northern Greece.
- Shokrollahi, M., Ebadi, H., & Sahebi, M.R. (2014). Fusion of PolSAR and Hyperspectral Images for Land Cover Classification. M.Sc. Thesis in Surveying Engineering and Photogrammetry, *K.N. Toosi University of Technology Faculty of Geodesy and Geomatics*.
- Silva, E.A., & Clarke, K.C. (2002). Calibration of the SLEUTH urban growth model for Lisbon and Porto, Portugal. *Computers Environment and Urban Systems*, 26(6): 525 – 552.
- Townshend, J.R.G., Justice, C.O., Gurney, C., & McManus, J. (1992). The impact of misregistration on change detection, in *IEEE Transactions on Geoscience and Remote Sensing*, vol. 30, no. 5, pp. 1054-1060.
- Xie, M., & Fu, M. (2011). The temporal dynamics of urban heat islands derived from thermal remote sensing data by local indicator of spatial association in Shenzhen, China. *Paper presented at the International Conference on Photonics and Image in Agricultural Engineering (PIAGENG 2010)*.
- Yousif, O., & Ban, Y. (2017). Fusion of SAR and Optical Data for Unsupervised Change Detection: A Case Study in Beijing. *Joint Urban Remote Sensing Event (JURSE)*.
- Zeng, Y., Zhang, J., & van Genderen, J. L. (2008). Change detection approach to SAR and optical image integration. *International Society for Photogrammetry and Remote Sensing*, 1077-1083.
- Zhang, B., Chen, K., Zhou, Y., Xie, M., & Zhang, H. (2010). Research on Change Detection in Remote Sensing Images by using 2D-Fisher Criterion Function Method. *ISPRS TC VII Symposium, 00 Years ISPRS, Vienna, Austria, July 5–7, Vol. XXXVIII, Part 7B*.